COMPUTATION OF DIMENSIONLESS SPECTRUM OF FLUID FORCES INDUCED BY VORTEX SHEDDING FROM A SINGLE RIGID TUBE IN A SINGLE-PHASE CROSS FLOW.

François JUSSERAND
Electricité De France –R&D Division
Fluid Mechanics, Power Generation and Environment
6, Quai Watier
78400 CHATOU, FRANCE
francois.jusserand@edf.fr

André ADOBES
Electricité De France –R&D Division
Fluid Mechanics, Power Generation and Environment
6, Quai Watier
78400 CHATOU, FRANCE

Thomas PASUTTO
Electricité De France –R&D Division
Fluid Mechanics, Power Generation and Environment
6, Quai Watier
78400 CHATOU, FRANCE

Lisette BROUTIN
ECOLE CENTRALE DE MARSEILLE
Technopôle de Château-Gombert
38, rue Frédéric Joliot Curie
13451 MARSEILLE, Cedex 20

ABSTRACT

Computation of the dynamic response of a structure submitted to a fluid flow requires the knowledge of the spectrum of fluid forces acting on the structure. In order to get that spectrum, one usually proceeds by rescaling a dimensionless envelope spectrum, which has been previously elaborated by applying safety margins to the most conservative of all spectra derived from a set of scaled experimental configurations.

When designing nuclear steam generator tube bundles to minimize flow-induced vibrations, one of the most popular dimensionless envelope spectra is the one proposed by Axisa et al.*.(1985,1990) In his papers, Axisa proposed a method that allows one to experimentally derive the dimensionless spectrum as a function of a dimensionless parameter, the "reduced frequency".*

Although Axisa initially applied his method to derive turbulent buffeting forces, we here propose to use it to derive the dimensionless spectrum of fluid forces due to vortex shedding. We consider the case of a single rigid tube in an upwards water cross-flow. Tube wall fluid stresses are derived by using Code_Saturne® *which is EDF CFD reference code.*

The paper includes four parts.

In the first part, we present the two laboratory configurations "AMOVI" and "DESider", which provide the experimental data used in the framework of the present study..

In the second part, we detail the post-processing that we used to derive the dimensionless spectrum from the computed tube wall fluid stresses.

In the third part, we validate the CFD simulations on the basis of the "DESider" air case, for which several fluid dynamics experimental results are available.

In the fourth part, we post-process tube wall pressures to derive the fluid force dimensionless spectrum in the "AMOVI" water case. We also perform a sensitivity study of our results, with respect to both boundary conditions and Reynolds number value. Numerical methodology allows one to readily distinguish the drag from the lift component in the overall fluid force.

1. INTRODUCTION

In nuclear plants, steam generator tubes might fissure or even break for vibratory reasons, as a consequence of excitation by the secondary fluid flow. Such tube damages would at once induce leakage of radioactive primary fluid into the secondary circuit, potentially affecting environment. That threat being a major concern for plant operators such as EDF, important research efforts have been devoted in the last decades to improve the knowledge of fluid forces.

Fluid forces are however governed by complex physics, which combines fluid-structure interaction and two-phase thermal-hydraulics. Their derivation has thereafter been essentially based on experimental results obtained on scaled test-facilities.

Improvement of Computational Fluid Dynamics (CFD) codes as well as growth of High Performance Calculation (HPC) more and more suggest that CFD codes could in the next decades become a useful tool to support and complement our empirical knowledge of fluid forces.

Our ultimate goal is the modelling of a full U-tube bundle dynamics coupled to a two-phase high void fraction secondary fluid flow in real operating conditions. This calculation is still quite too complex. Thus, in the present paper we start with the simulation of simple laboratory cases, based on arrangements of straight tubes submitted to single phase cross-flows in rectangular channels.

Moreover, one may categorize fluid forces into three classes which respectively include "fluid-elastic" forces, random turbulent forces, and forces due to vortex shedding from tubes. Fluid forces associated with two-phase flow are far more difficult to model than the ones associated with single phase flow.

In that context, the present paper focuses on the computation of fluid forces due to vortex shedding of a single rigid tube submitted to a single-phase cross flow in a rectangular channel.

2. NOMENCLATURE

Greek alphabet

$\underline{\underline{\sigma}}$	Fluid stress tensor
ϕ'	Autocorrelation spectrum
γ	Coherence function
δ_{ij}	Kronecker delta
ρ	Density
$\underline{\underline{\tau}}$	Viscous stress tensor
λ_c	Correlation length
ψf_{lin}	Cross-correlation spectrum of linear load density vector

Latin alphabet

D	Tube diameter
f	Frequency
f_r	Reduced frequency
f_{lin}	Linear load density vector
F_k	Fluid force of k^{th} face
H	Mock-up height
L	Mock-up length
N_{b_i}	Mesh faces number at abscissa s_i
$R_{f_{lin}}$	Cross-correlation function
R_e	Reynolds number
s	Abscissa along tube axis
s_i	Mesh abscissa at section "i"
S_t	Strouhal number
t	Time
V_0	Inlet velocity
V_g	Gap velocity
X	Position vector
x_i	i^{th} component of x

Superscripts

t	Transpose

Subscripts

i,j,k	Vector, tensor components or face or section number
$drag$	Drag direction
$lift$	Lift direction

3. LABORATORY CONFIGURATIONS UNDER STUDY

AMOVI is an evolutionary mock-up that was built by the French Commissariat à l'Energie Atomique (CEA). Its simplest configuration, consists of a single rigid straight cylindrical tube submitted to an upwards water cross-flow in a rectangular channel (Figure 1 and Table 1)

DESider is the acronym standing for the name of a European project, "*D*etached *E*ddy *S*imulation for *In*dustrial A*er*odynamics". In that context, a mock-up was used by Braza *et al.*(2003) in order to get PIV measurements downstream of a single fixed rigid tube submitted to an horizontal air cross-flow in a rectangular channel (Table 1). In the following, DESider refers to this test facility.

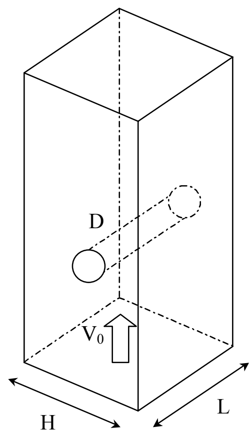

Figure 1*: Diagram of AMOVI test facility*

AMOVI and DESider main characteristics are given in table 1, where Reynolds number Re, based on inlet velocity, is computed as : $Re = \frac{V_0 D}{\upsilon}$

	AMOVI	DESider
Fluid	water	air
L (m)	0.1	0.67
D (m)	$12.15\ 10^{-3}$	0.14
H (m)	0.07	0.67
V_0 (m/s)	10	15
Re	121500	139691
Fluid cross flow	upwards	horizontal

Table 1: AMOVI and DESider test-facilities main characteristics

4. NUMERICAL METHOD

4.1 Computation of tube wall excitations

Single-phase fluid (water in the case of AMOVI and air in the case of DESider) is assumed to be incompressible and Newtonian. Fluid dynamics calculations are performed by using EDF *Code_Saturne*® CFD code, which allows one to solve Navier-Stokes' equations on unstructured meshes (Archambeau *et al.,* 2004)

Code_Saturne® is based on a collocated finite volume approach. Momentum equations are solved considering an explicit mass flux. Velocity and pressure coupling is insured by a SIMPLEC prediction/correction method with outer iterations.
For the U-RANS calculations presented hereafter, second order schemes are used in space (centred with slope test for all the variables), and a first order implicit scheme is used in time. As a first step of our methodology, we used two equations U-RANS model, "k-ω SST" model, being only interested in unsteady coherent structures.

4.2 From tube wall excitations to dimensionless fluid forces spectrum

The cylinder being rigid, wall excitation forces exclusively on fluid dynamics, using CFD computations. They are post-processed in the frame of experimental methodology suggested by Axisa *et al.*(1985,1990) in order to derive the dimensionless spectrum of fluid forces.

A specific hexahedral mesh of the fluid domain is elaborated. Tube wall is subdivided into elementary "cylindrical surfaces", and each of those elementary surfaces is subdivided into "elementary faces" (figure 2).

Code_Saturne® provides tube wall stress tensor $\underline{\underline{\sigma}}_i^k(t)$ at time t, at the centre of each elementary face k of elementary cylindrical surface i. An elementary vector force $F_i^k(t)$ is then derived from $\underline{\underline{\sigma}}_i^k(t)$:

$$F_i^k(t) = \int_{S_i^k} \underline{\underline{\sigma}}_i^k(t)\,\vec{n}\,d S_i^k \qquad (1)$$

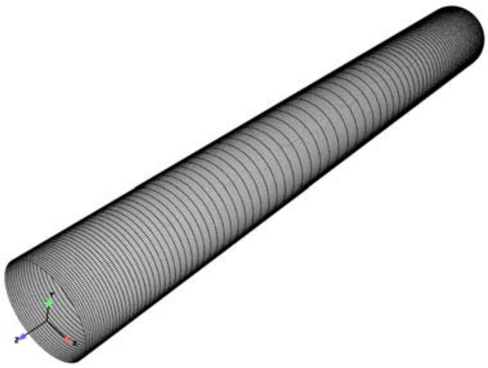

Figure 2 *:Tube wall surface mesh*

Where $\vec{n}$ denotes normal unit vector associated to elementary surface S_i^k. Post-processing first step consists in calculating $f_i(t)$, the force per unit length exerted on elementary cylindrical surface number *i*, whose center is situated at abscissa s_i. Let Nb_i denote the number of elementary faces which compose cylindrical surface number *i* :

$$f_i(t)=\sum_{k=1}^{Nb_i}\left[F_i^k(t)\right] \qquad (2)$$

Once the $f_i(t)$ have been derived for all the elementary cylindrical surfaces that compose the tube wall, cross-correlation spectrum $\psi_f(s_i,s_j,f)$ between any couple of them can be computed as the Fourier transform of their cross-correlation function.

$$R_{ij}^f(\varsigma) = \lim_{T\to\infty} \frac{1}{T}\int_0^T f_i(t).f_j(t+\varsigma)dt \qquad (3)$$

$$\psi_f(s_i,s_j,f) = \int_{-\infty}^{+\infty} R_{ij}^f(\varsigma)\,e^{-2i\pi f \varsigma}d\varsigma \qquad (4)$$

Where R_{ij}^f denotes cross-correlation function of forces per unit length between locations s_i and s_j.

$\psi_f(s_i,s_j,f)$ is then scaled using the following scaling factors :

- velocity is scaled using gap velocity, $V_g = V_0\dfrac{H}{H-D}$, where V_0 denotes upstream flow velocity, H is channel height, and D tube diameter.
- $f_i(t)$ is scaled using permanent force density, $\Gamma = \dfrac{1}{2}\rho V_g^2 D$, where ρ is the volumetric mass of the fluid.

Let us introduce reduced frequency $f_r = \dfrac{fD}{V_g}$.

$$\overline{\Psi}_f(s_i,s_j,f_r) = \left(\frac{1}{2}\rho V_g^2 D\right)^{-2} \frac{V_g}{D} \psi_f(s_i,s_j,f_r) \qquad (5)$$

Assuming that the tube is excited by a uniform cross-flow, the fluctuations are not conveyed along the tubes. One can thus write cross-correlation spectrum as :

$$\overline{\Psi}_f(s_i,s_j,f_r) = \phi'(f_r)\gamma(s_i,s_j) \qquad (6)$$

Where $\phi(f_r)$ denotes autocorrelation spectrum of turbulent fluid forces per unit tube length.

γ denotes the coherence function, which characterizes the degree of spatial correlation of forces along the tube. γ, and is usually approximated by :

$$\gamma(s_i,s_j) = exp\left\{-\frac{\left|s_i - s_j\right|}{\lambda_c}\right\} \qquad (7)$$

Where correlation length λ_c is about a few tube diameters according to experimental evidence.

5. VALIDATION ON FLUID DYNAMICS COMPUTATIONS ON THE BASIS OF THE “DESider” CASE

In order to validate fluid dynamics computations, the “DESider” case is first considered (simulated). Two criteria are chosen to validate calculations convergence : mean velocity field and Strouhal number S_t.

The mesh for the fluid domain has been proposed by Braza *et al.*(2003). A total of approximately 2 M cells are thereafter used in the computations. The mesh used is unstructured and composed of several conforming blocks. Its refinement around the tube is more important than elsewhere, since vortex shedding frequency is one of the criteria of calculations convergence.

A y^+ value in-between 5 to 10 is reached in the first cell layer near channel and tube walls. Preliminary tests have been performed to optimize the time step value which is around 10^{-5} s. Courant Number value thereafter rounds unity.

An inlet boundary condition is imposed to fluid flow at one side of the domain, and an outlet boundary condition at the opposite side. Wall conditions are imposed elsewhere.

About 45000 iterations are needed to reach a converged solution, using 32 processors of one of EDF cluster machines.

Figures 3 and 4 allow one to compare Braza’s experimental mean velocity fields (Braza *et al.*, 2003) to those computed with *Code_Saturne*®.

One can appreciate that CFD results are quite similar to those measured on Braza’s mock up.

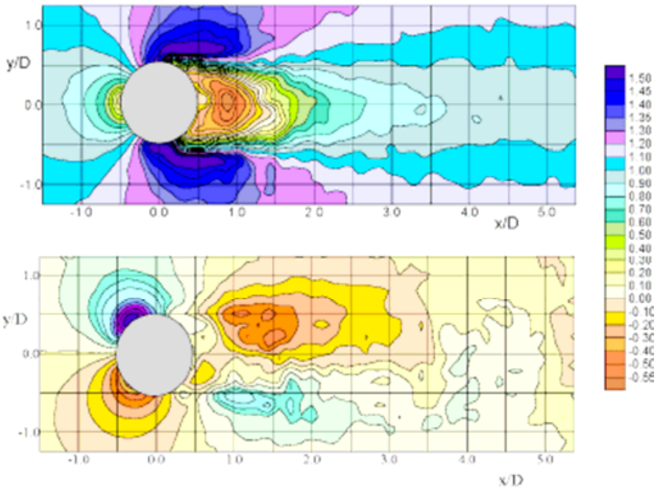

Figure 3 : *Braza’s Particle Image Velocimetry measurements : components of mean velocity along drag (upper graph) and lift directions (lower graph)*

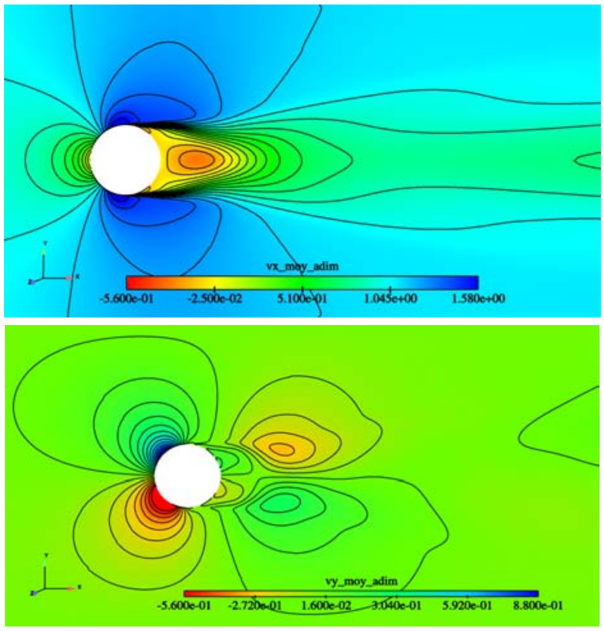

Figure 4 : *Computation results : components of mean velocity along drag (upper graph) and lift directions (lower graph)*

Strouhal number S_t is a dimensionless parameter based on Von Karman streets frequency. Experimental value of S_t (0,21) is close to the one derived from computations (0,25). That difference could be due to the difference in wall roughness between test facility and calculations. According to Blevins, Strouhal number is indeed slightly higher with rough tubes than it is with smooth ones (Blevins *et al.,* 2001). Walls are supposed to be smooth in the numerical model, whereas they are rough in Braza’s mock up.

6. RESULTS AND SENSITIVITY ANALYSIS

Since Reynolds numbers are similar in DESider and AMOVI experiments (table 1), the meshes used to model the two experiments are similar, too. In AMOVI computation, y^+ values in-between 1 and 15 are reached in the first cells layer around the tube. Fluid boundary conditions are the same in both computations.

The time step and the number of iterations must be chosen with care. Courant number values around the unity have also to be reached. On the one hand, one has to fulfill all criteria imposed by calculations' numerical convergence. On the other hand, one has to pay attention to standard signal processing criteria (Shannon criterion, windowing…) required for spectrum derivation : high observation limit frequency and fine frequency resolution are required to make derived spectrum as informative as possible.

Former parameter is related to calculations time step, while latter parameter depends on duration of signal simulation, once the non stationary converged solution has been reached. After preliminary tests, time step is chosen equal to 10^{-5} s, corresponding to a sampling frequency of 10 000 Hz. Duration of signal simulation is chosen equaling 0.5 s, corresponding to a frequency resolution of 2 Hz. In the case of a 4.0 m/s upstream velocity, twenty thousand iterations are required to reach the converged solution.

Four upstream velocities are considered : 4.0, 6.0, 8.0 and 10.0 m/s.

Figure 6 displays dimensionless auto-spectrum computed along drag and lift directions versus reduced frequency at a 121500 Reynolds number. Main characteristics of the spectrum are the same along both directions. One can observe a region of high energy fluid excitation at low frequencies and a region of decaying fluid excitation. In a logarithmic axis system, auto-spectrum decreases with reduced frequency f_r according to a "- 3.5" slope.

In lift direction, spectrum is characterized by a peak (f_r=0.26) associated to von Karman streets frequency. In drag direction, the same kind of phenomenon is observed but peak is lower and its frequency is twice the one of von Karman streets.

Considered Reynolds' number range ($300 < Re < 1.5x10^5$) is called sub-critical. In that range, vortex shedding is strong and periodic.

A sensitivity study was then performed. Input parameters of that study were boundary conditions applied to the fluid on lateral channel walls as well as Reynolds number value.

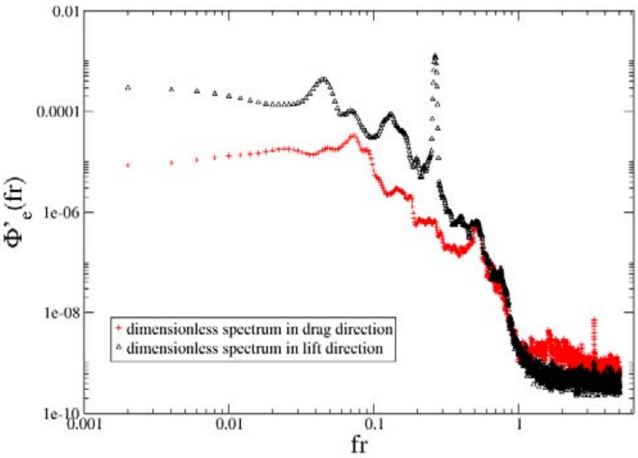

Figure 5 *: Dimensionless spectra (in drag and lift directions) versus reduced frequency with Re=121 500*

Standard wall boundary conditions on channel walls perpendicular to cylinder axis were replaced by "periodic" boundary conditions, so that the simulated configuration could be considered as the one of an infinite cylinder in a channel infinitely large along tube axis. Figures 6 and 7 present the results of those calculations.

First of all, energy spectrum level is lower in the case of periodic conditions. Energies at peak values are nonetheless slightly the same at frequency peak values, i.e. at dimensionless vortex shedding frequency in lift direction, and at twice that frequency in drag direction.

Those results show the influence of wall conditions on energy spectra. Important re-circulations due to wall conditions occur in tube direction, downstream the cylinder. According to spectra comparison (figures 6 and 7), frequencies corresponding to those vortices are low and convey much energy, compared to the case of the "infinite tube". Analysis of spectra per elementary cylindrical surface shows that spectra shapes are the same for the two types of boundary conditions beyond some distance *"d"* from the wall. The order of magnitude of *d* is 2*D*, where *D* denotes tube diameter.

Influence of Reynolds number was also studied in the frame of standard wall conditions. Four values of Reynolds number were used, rounding

48000, 73000, 97000, 121000

Spectrum shapes are about the same in the four computations. As far as peak values are concerned, reduced frequencies slightly vary from one case to another but energy peak value does not change. For low frequencies, excitation energy slightly increases with Reynolds number. As previously shown, this range of frequencies is related to wall re-circulations vortices. As fluid incident velocity is different, those vortices do not have the same energy. The higher the Reynolds number, the bigger vortices energy. Resulting value of energy ratio between extreme cases in that low frequency region is about one decade.

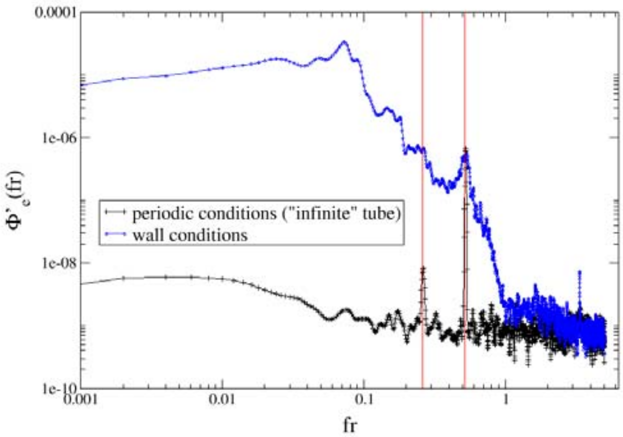

Figure 6*: Influence of boundary conditions on dimensionless spectrum in drag direction*

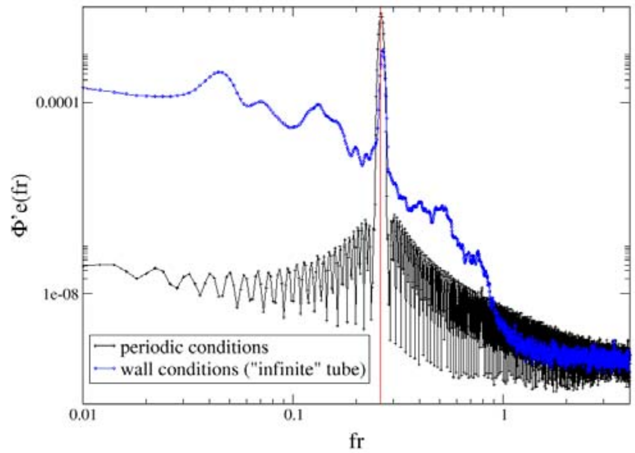

Figure 7 *: Influence of boundary conditions on dimensionless spectrum in lift direction*

7. CONCLUSION

Axisa's method was applied to compute the dimensionless spectrum of fluid forces due to vortex shedding from a single rigid tube in an upwards water flow. Tube wall stresses that are necessary to apply that method were obtained using *Code_Saturne*® which is EDF CFD code.

CFD simulations based on the "k-ω SST" turbulence model have first been validated on the basis of DESider project measurements. Tube wall fluid stresses post-processing has then been improved on the basis of the AMOVI mock up. This entirely numerical methodology has now to be tested on more complex cases, including for instance tube bundles and two-phase flows. A U-RANS approach such as the one applied in the present paper allows one to study fluid excitations due to unsteady coherent structures. Further research is now planned, to consider fluid excitations due to turbulent random fluctuations using the LES approach (Elmiligui *et al*., 2004) .

8. REFERENCES

ADOBES, A., PILLET, J., GAUDIN, M., 2006, Influence of fouling and plugging on the stability diagram of nuclear plants. In *Proceedings of the Pressure and Vessel Pipe International Conference.*

ARCHAMBEAU, F., MECHITOUA, N., SAKIZ, M., 2004, Code_Saturne : a Finite Volume Code for the Computation of Turbulent Incompressible Flows – Industrial Applications. *International Journal on Finite Volumes,* Vol.1.

AXISA, F., ANTUNES, J., VILLARD, B., 1990, Random Excitation Of Heat Exchangers Tubes By Cross-flow. *Journal of Fluids and Structures*, Vol. 4, pp. 321-341.

AXISA, F., VILLARD, B., GIBERT, R.J., BOHEAS, M.A., 1985, Vibration of tube bundles subjected to steam-water cross-flow *Proceedings of the 8th International Conference on Structural Mechanics in Reactor Technology.*

BLEVINS, R.D., 2001, Flow-Induced Vibration. *Krieger Publishing Company*.

DJERIDI, H., BRAZA, M., PERRIN, R., HARRAN, G., CID, E., CAZIN, S., 2003, Near-wake turbulence properties around a circular cylinder at high Reynolds number, *J. Flow Turbulence and Combustion*, **71**, 19-34.

Elmiligui, A., ABDOL-HAMIDT, K.S., MASSEY, S.J., PAO, S.P., 2004, Numerical Study of Flow Past a Circular Cylinder Using RANS, Hybrid RANS/LES and PANS Formulations. In *22nd Applied Aerodynamics Conference and Exhibit*.

INADA, F., YONEDA, K., YASUO, A., NISHIHARA, T., 2007, A Study on Fluid Excitation Forces Acting on a Rotated Square Tube Bundle of T/D=3.1 in Cross-Flow. In *Proceedings of ASME*, Vol. 129, pp. 162-168.